The electronic properties of polythiophene

1992 J. Phys.: Condens. Matter 4 101

(http://iopscience.iop.org/0953-8984/4/1/021)

J. Phys.: Condens. Matter 4 (1992) 101–120. Printed in the UK

The electronic properties of polythiophene

Michael Springborg†

Nordisk Institut for Teoretisk Atomfysik (NORDITA), Blegdamsvej 17, DK 2100 København Ø, Denmark

Received 2 November 1990, in final form 10 May 1991

Abstract. Electronic ground-state properties of planar, periodic, infinite polythiophene chains are calculated using a first-principles, density-functional method. We concentrate on a set of geometries differing in the size of the carbon–carbon bond length alternation along the backbone, thus studying a transition between a quinoid and an aromatic structure. Whereas the lowest unoccupied orbitals are found to have π symmetry we find valence energy bands of σ symmetry unusually close to the Fermi level. It is demonstrated that the valence band structures offer a consistent interpretation of experimental photoelectron spectra. An important result is the lack of a band-gap closure when passing from the aromatic to the quinoid structure, although the band gap is diminished. The results are used in deriving a model Hamiltonian with which we subsequently study the π-electron density of states for solitonic and polaronic excitations. The above-mentioned lack of band-gap closure leads to the absence of near-mid-gap states for solitons. Polarons induce states asymmetric in the gap and, comparing with experimental results for doped and photo-excited polythiophene, we estimate the width of the polaron to be large (of the order of eight thiophene units which, however, might be slightly modified when including correlation effects), and we suggest that bipolarons and not polarons are the charge carriers in doped polythiophene in the dilute limit.

1. Introduction

In the course of exploring the properties of the carbon-based conjugated polymers polythiophene plays a central role (see, e.g., reference [1]). Compared with the prototype of the conjugated polymers, *trans* polyacetylene, polythiophene shows both similarities and differences which make a detailed study of polythiophene itself and a comparison with *trans* polyacetylene useful and interesting. Among the common properties is the large doping-induced increase in electrical conductivity [2, 3]. The important advantages of polythiophene over *trans* polyacetylene include its stability towards atmospheric exposure [4] and thermal treatment [5], the possibility of forming highly crystalline compounds [6] as well as soluble materials when substituting (some of) the hydrogen atoms with other sidegroups [7].

As for *trans* polyacetylene, the C–C–C bond angles for polythiophene (figures 1(*a*) and 1(*b*)) are close to 120°, and one may consider polythiophene a modification of *trans* polyacetylene for which the carbon backbone possess a slightly more complicated

† Present address: Fakultät für Chemie, Universität Konstanz, W 7750 Konstanz, Federal Republic of Germany.

0953-8984/92/010101+20$03.50

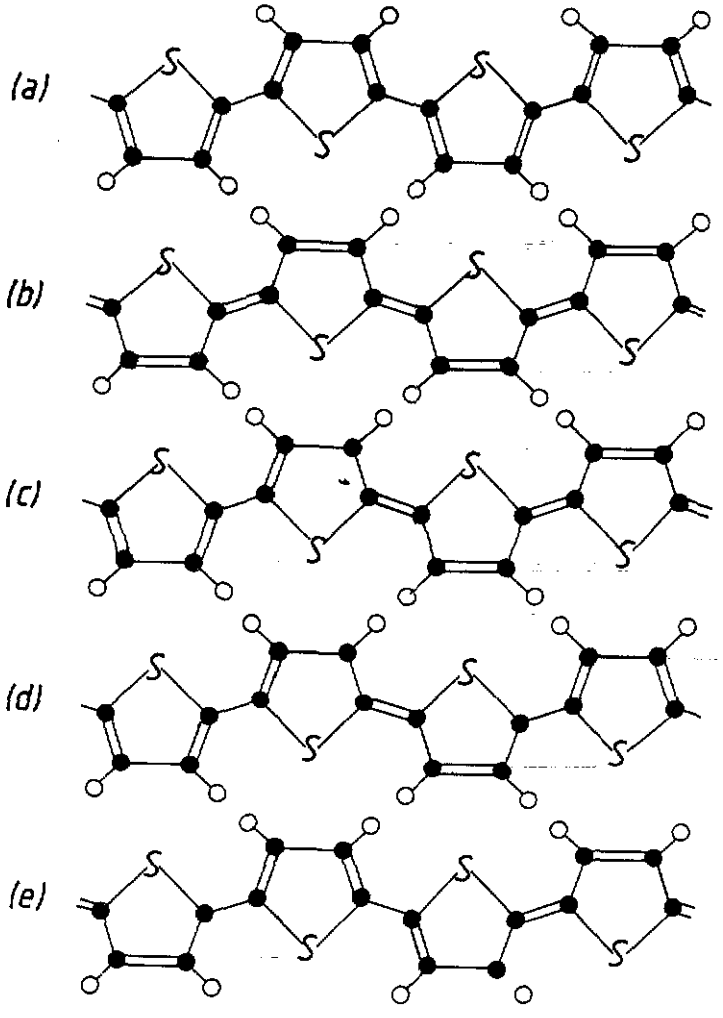

Figure 1. Schematic representation of (*a*) aromatic and (*b*) quinoid polythiophene. Also shown is (*c*) a soliton in polythiophene as well as a polaron in (*d*) aromatic polythiophene, and in (*e*) quinoid polythiophene. The full and open circles represent carbon and hydrogen atoms, respectively, whereas the sulphur atoms are represented by the letter S.

structure and where certain pairs of hydrogen atoms have been replaced by single sulphur atoms.

Interchanging the double and single bonds in *trans* polyacetylene results in an energetically equivalent structure. The two forms are denoted the A and the B phase, respectively. Domain walls (solitons) separating the A and the B phases of single chains have been proposed [8,9], responsible for the large doping-induced increase in electrical conductivity for *trans* polyacetylene. However, the energetical degeneracy of the A and B phases is specific for *trans* polyacetylene and the A and the B phases for polythiophene—the aromatic and the quinoid structure shown respectively in figures 1(*a*) and 1(*b*)—are energetically slightly different, and solitons (figure 1(*c*)) may therefore be unstable. Polarons (figures 1(*d*) and 1(*e*)) have therefore been

argued to be the charge carriers in a number of doped conjugated polymers including polythiophene [10–12].

Within this picture the conducting properties of polythiophene can be described by only the geometrical structure of the underlying carbon backbone plus the carbon-centred π orbitals, and one may therefore ask whether the sulphur atoms actually do play such a secondary role. It is one purpose of this paper to explore this question.

We have studied ground-state properties of isolated, infinite, periodic, planar chains of polythiophene using a first-principles, density-functional method. This method has been described in detail elsewhere [13,14] and is therefore discussed only briefly in section 2. The results of the first-principles calculations are reported in section 3 where they are also compared with experimental and other theoretical results. Based on these results we discuss in section 4 a model Hamiltonian with which in section 5 we examine solitons and polarons. Finally, section 6 contains the conclusions.

2. The first-principles method

We make use of the Born–Oppenheimer approximation and of the Hohenberg–Kohn density-functional formalism [15] with the local approximation of von Barth and Hedin [16]. The eigenfunctions to the single-particle Kohn–Sham equations [17] are expanded in a basis of linear muffin-tin orbitals (LMTOs).

In the present approach the basis set consists of two subsets, each containing s, p and d functions on all sites but differing in the decay constants in the interstitial region. We assume the polymer chain to be infinite and periodic and make use of the zigzag symmetry. Each unit cell of polythiophene contains accordingly one C_4H_2S unit. A dimensionless k variable with $k = 0$ and $k = 1$ being the zone centre and the zone edge, respectively, is introduced.

In examining the planar chains of figures 1(a) and 1(b) we split the basis functions into being either symmetric (σ) or antisymmetric (π) with respect to reflection in the plane of the nuclei. Because of numerical instabilities, due to almost linear dependencies of the basis functions, we contract each subset using a canonical transformation [18] whereby those linear combinations corresponding to the smallest eigenvalues of the overlap matrix are excluded. Polythiophene is the largest system so far examined with the present method, and it turns out that there are non-negligible linear dependences which are most pronounced for the functions of σ symmetry. This forces a stronger contraction of the σ functions than of the π functions, which in turn leads to a shift of the σ single-particle energies relative to the π single-particle energies, as we shall see. We mention that similar behaviour has not been observed for systems with smaller unit cells.

It should finally be stressed that our (parameter-free) approach includes correlation effects and that we have used the muffin-tin approximation solely in defining the basis functions. Moreover, throughout the paper we assume $T = 0$ and thus neglect temperature and entropy effects.

3. First-principles results

The internal geometries of charged chains with polaronic or solitonic distortions are dictated by very small differences in the total energy. These can, for example, be

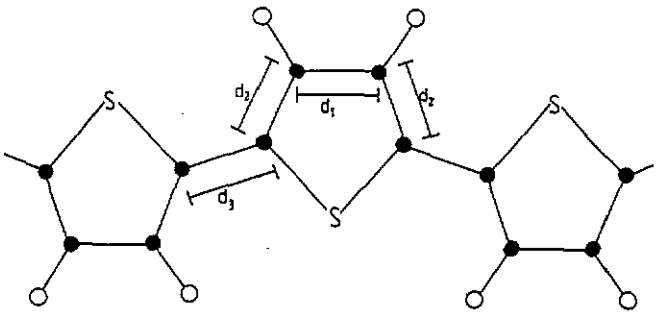

Figure 2. The notation of the carbon–carbon bond lengths.

estimated from calculations with model Hamiltonians for which the parameters are obtained from detailed calculations on periodic, infinite, neutral chains where all geometrical parameters are allowed to relax. With the present method this is an almost impossible task to carry through for polythiophene with its seven atoms per unit cell. We have therefore decided to use a much simpler approach, believing that the results will throw some light upon the properties of charged polythiophene chains but simultaneously realizing that the results might not be definitive.

The bond lengths d_1, d_2, and d_3 (see figure 2) have previously been optimized using the semi-empirical MNDO (modified neglect of diatomic overlap) method and found to be around 2.73 au, 2.61 au, and 2.73 au, respectively, for the aromatic structure and about 2.56 au, 2.78 au, and 2.56 au, respectively, for the quinoid compound [19,20]. We will therefore vary d_1, d_2 and d_3 as

$$\begin{aligned} d_1 &= (2.645 + \delta 0.085)\ \text{au} \\ d_2 &= (2.695 - \delta 0.085)\ \text{au} \\ d_3 &= (2.645 + \delta 0.085)\ \text{au} \end{aligned} \tag{1}$$

with δ being the only parameter to vary. Furthermore, we fix the C–H bond lengths at 2.05 au, and place the hydrogen atoms along the negative C–C–C bond angle bisectors. The C–S–C bond angles are set equal to 92°, the C–S bond lengths to 3.245 au, and the C–C bonds with lengths d_3 are assumed to make an angle of 120° with the neighbouring C–S bonds. According to the results of the MNDO calculations [19,20] this results in reasonable structures. It should be added that the aromatic structure is believed to be the ground-state structure for the neutral chain. (See, e.g., [6,20].)

In figure 3 we show our calculated band structures for the structure with $\delta = 0$. We notice the surprising finding of orbitals of σ symmetry being those defining the top of the valence bands, but notice also that the uppermost valence orbitals of π symmetry have only slightly lower energies. On the other hand, the bottom of the conduction bands is clearly defined by orbitals of π symmetry, and the lowest-lying conduction orbitals of σ symmetry (not shown) are found for positive band energies. The first finding might be related to the above-mentioned different contractions of the σ and the π basis functions such that we cannot exclude a relative shift of the π and σ energy bands. We shall return to this point below.

In table 1 we list some key quantities as obtained with the present method for the quinoid structure ($\delta = -1$), the 'undimerized' structure ($\delta = 0$), and the aromatic

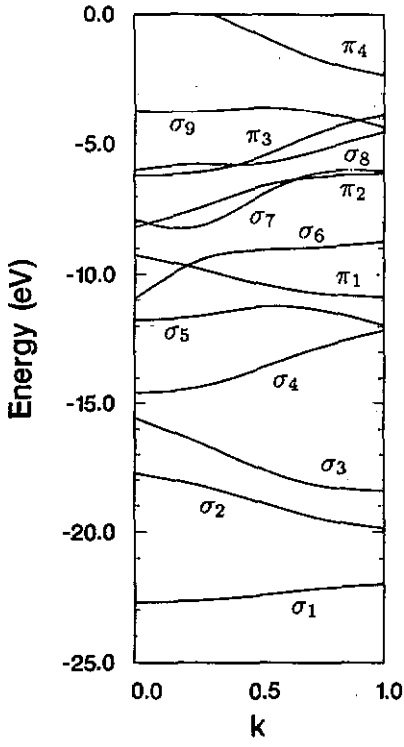

Figure 3. The first-principles band structures for periodic polythiophene with $\delta = 0$. The unit cell contains one C_4H_2S unit, and $k = 0$ and $k = 1$ corresponds to the zone centre and zone edge, respectively. The broken line represents the Fermi level.

structure ($\delta = +1$) together with results of other theoretical and experimental studies of polythiophene. Our total valence band width (W) agrees reasonably with that found by the only other density-functional calculations on polythiophene [20]. On the other hand, the semi-empirical valence-effective Hamiltonian (VEH) method [21], as well as the *ab initio* Hartree–Fock method [22] overestimate the band width W.

Most often, a translational unit is used as the unit cell, which corresponds to doubling our unit cell and hence to folding the band structures of figure 3 about $k = 0.5$. Therefore, the width of the uppermost π valence band (W_π) may be related to only that part of the π_3 band in figure 3 for which $0.5 \leqslant k \leqslant 1.0$. This explains why one of the VEH studies [23] gives a significantly larger value of W_π than the other ones [21,24–27], and furthermore makes a direct comparison of the different values of W_π difficult. Nevertheless, the other density-functional values [20], which were found for helical symmetries, agree well with ours, whereas the VEH and *ab initio* Hartree–Fock methods seem to give too large a value for W_π.

Our value of the energy gap (E_G) for the aromatic structure agrees well with the experimental values [12,27], whereas the density-functional value of Mintmire *et al* [20] suffers from the typical density-functional underestimation. That we do not find this might be due to the lack of a geometry optimization. Otherwise, our results as well as those of Mintmire *et al* [20] and the Hückel results of Lee and Kertész [19] show that the aromatic structure has a significantly larger gap than the quinoid structure. We also notice that the *ab initio* Hartree–Fock calculations [22,28]

Table 1. The total valence band width (W), the width of the uppermost π valence band (W_π), the ionization potential (the negative of the energy of the uppermost occupied orbital, IP), and the optical $\pi_3 \rightarrow \pi_4$ gap (E_G) in eV as found by various theoretical and experimental methods. The quinoid, aromatic and undimerized structures correspond to $\delta = -1$, $+1$, and 0, respectively, and the applied methods include Hückel, local-density (LDF), VEH, *ab initio* Hartree–Fock (*ab initio* HF), and CNDO calculations as well as optical absorption (Opt. Abs.) and photoelectron emission (Phot. Em.) spectroscopy experiments. It should be noticed that some of the values of W_π correspond to a translational symmetry, whereby only the upper half of the π_3 band of figure 3 is considered. Finally, the aromatic structure was considered in the theoretical studies when nothing else is mentioned.

W	W_π	IP	E_G	Comment	Reference
19.1	2.9	3.5	1.1	Quinoid	Present work
18.8	2.4	3.8	1.7	Undimerized	Present work
18.4	1.9	3.9	2.1	Aromatic	Present work
			0.5	Hückel, Quinoid	[19]
			1.8	Hückel, Aromatic	[19]
21	~ 3	2	0.2	LDF, Quinoid	[20]
20	~ 2.5	2.5	1.7	LDF, Aromatic	[20]
28	2.6	5.0	1.6	VEH	[21]
27	2.9	9.5	8.1	*ab initio* HF	[22]
	4.5	5.3	2.2	VEH	[23]
			2.2	VEH	[24]
	2.4	5.1	1.7	VEH	[25]
	2.6	5.0	1.6	VEH	[26]
	2.5		1.9	VEH	[27]
	4.0	8.3	7.6	CNDO	[30]
			1.7	Hückel	[31]
	2.8	9.6	7.6	*ab initio* HF	[28]
			2.0	Opt. Abs.	[12]
			2.0	Opt. Abs.	[27]
		5.5		Phot. Em.	[33]
		5.3		Phot. Em.	[38]

and the semi-empirical CNDO (complete neglect of differential overlap) calculations [29,30] lead to a large overestimate in the gap, whereas the values found in the VEH calculations are surprisingly close to the experimental value. Also the Hückel calculations on helical polythiophene [31] result in a realistic gap.

One important result of our calculations is that as a function of δ we do not find any band-gap closure when passing from the aromatic to the quinoid structure. This is in disagreement with the semi-empirical results of Mintmire *et al* [32].

Onoda *et al* [33] have experimentally studied photoelectron emission spectra of polythiophene. They find the top of the valence band to lie at about -5.5 eV, i.e. about 2 eV below our value, even more below the value of Mintmire *et al* [20], but about 4 eV above the value of Bakhshi *et al* [22] and Otto and Ladik [28]. The VEH value of Brédas and co-workers is in good agreement with the experimental value, but has been adjusted by almost 2 eV.

The largest disagreement between our results and those of the other calculations concerns the question of the existence of an overlap between the highest valence π band and the σ bands. Except for the results of Tanaka *et al* no such overlap has been reported earlier. Also the density-functional results by Mintmire *et al* [20], with which ours should have the closest agreement, lack this overlap. Their σ valence

bands range from −23 eV to −7 eV, and their π valence bands span the range between −9 eV and −2 eV. We find the σ valence bands between −23 eV and −3 eV and the π valence bands between −11 eV and −3 eV. Our widths are thus larger which could be due to different convergences of the basis sets. One important difference between our calculations and those of Mintmire *et al* [20] is the lack of sulphur d functions in the latter. We have earlier [34–36] argued for their importance in describing the electronic properties of some sulphur-containing polymers. In the present calculations we find, however, their importance less pronounced although not negligible. The lack of these in most other calculations on polythiophene might therefore be a part of the reason for the discrepancy.

Wu *et al* [37] have reported both ultraviolet and x-ray photoelectron spectra (UPS and XPS, respectively) of polythiophene. Most detailed are the XPS results and since their UPS spectra do not show any important deviations from the XPS results we will concentrate on the latter and interpret their peaks as related to maxima in the density of states (DOS) thereby neglecting matrix-element effects.

In figure 4(*a*) we reproduce their XPS spectrum and show moreover our calculated DOS (figure 4(*b*)) for the bands of figure 3 and a modified DOS (figure 4(c)) in which the σ bands of figure 3 have been shifted 1 eV downwards. A comparison between figure 4(*a*) and figures 4(*b*) and 4(*c*) shows that figure 4(*c*) gives a better description of the spectrum than figure 4(*b*). The peak 20 eV below the Fermi energy ϵ_F is thus due to the σ_1 band, whereas the double peak at around 16 eV below ϵ_F originates from the σ_2 and σ_3 bands. The σ_5 and π_1 bands give rise to the double peaks at about 11 eV below ϵ_F, whereas the features 6–9 eV below ϵ_F are due to the σ_6 and σ_7 bands. Four bands (σ_7, σ_8, π_2, and π_3) are responsible for the features at 3–5 eV below ϵ_F. Finally, a weak shoulder at 1–2 eV below ϵ_F is attributed to the π_3 band by Wu *et al* but might also be due to the σ_9 band. This band has large sulphur p components and will therefore (as the π orbitals) be only slightly sensitive to x-ray photons.

Replacing every second hydrogen atom with a methyl group (CH_3) one arrives at poly-3-methylthiophene, which has very similar properties to the parent compound. This can, for instance, be seen from the UPS spectra of this polymer (Tourillon and Jugnet [30]) which can be interpreted according to the analysis above.

Very recently Fujimoto *et al* [38,39] reported UPS and MNDO studies of finite oligothiophenes with up to eight thiophene units. Since UPS spectroscopy has largest cross sections for orbitals with large p components this technique is particularly useful in studying π electrons of the macromolecules. Besides reporting a value of 5.3 eV for the ionization potential they reported two π bands in the uppermost part of the valence band region of which one increases its dispersion for increasing chain length; the other is narrow and placed at roughly 3.5 eV below ϵ_F. When neglecting the avoided crossing between the π_2 and π_3 bands we can interpret the bands as consisting of a hypothetical π_2(small k) + π_3(large k) band and a π_2(large k) + π_2(small k) band. Since the orbitals of the second band are mainly centred on the sulphur atoms and the so-called C_β sites (the carbon sites not neighbouring the sulphur atoms), these orbitals from different unit cells interact only little, and the resulting band is flat. This flat band is placed about 3 eV below ϵ_F in good agreement with the results of Fujimoto *et al* [38,39].

In total the analysis of the photoelectron spectra indicates that our σ bands have energies of about 1 eV too high relative to those of the π bands. But also with this modification an overlap between the π_3 and the σ_9 bands remains.

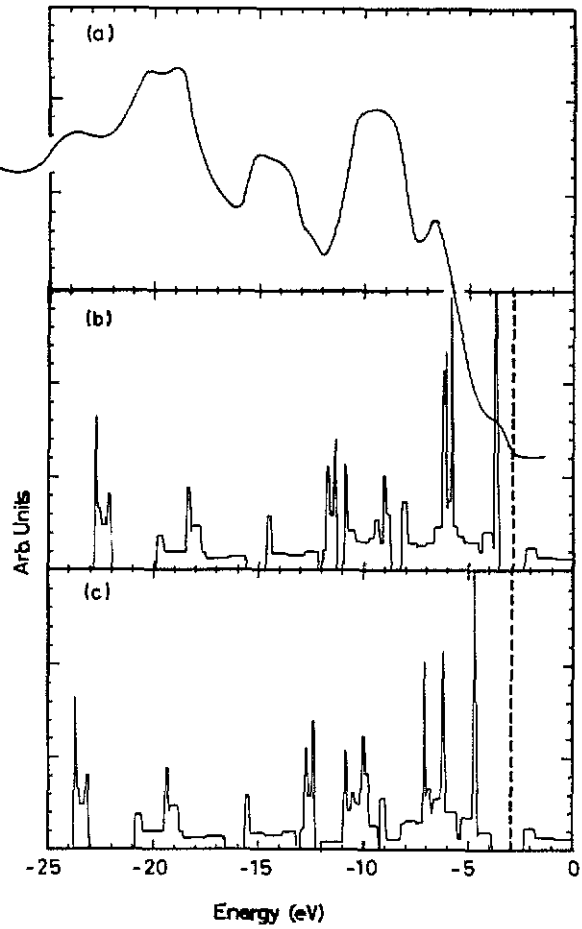

Figure 4. (*a*) Experimental XPS spectrum from reference [37]. (*b*) and (*c*) theoretical DOS curves. The σ bands have in (*c*) been shifted downwards by 1 eV. The vertical broken lines are the Fermi level.

XPS experiments on gaseous thiophene, C_4H_4S, have been reported by Derrick *et al* [40] and by Gelius *et al* [41]. The data were reported to agree well with the results of Hartree–Fock calculations, and as such interpreted showing that the two uppermost orbitals of the monomer have π symmetry. The *ab initio* Hartree–Fock calculations [42] gave π orbitals spanning 5.2 eV, and since Hartree–Fock calculations tend to overestimate band width a comparison with our total π valence-band width (8 eV) shows that the polymerization leads to a significant broadening. A similar broadening is to be expected for the σ bands and these will lead to a larger σ–π band overlap for the polymer than for the monomers.

Fink *et al* [43,44] have reported experimental electron energy-loss spectra for polythiophene. In the low-energy region the spectra of Fink [44] possess two peaks of which the lower-lying peak shows some dispersion as function of the momentum transfer q starting at energies of about 3 eV for $q = 0$, whereas the higher-lying peak is placed at about 4 eV, independently of q. Both peaks might be related to $\pi_3 \rightarrow \pi_4$ transitions but also $\sigma_9 \rightarrow \pi_4$ transitions can play a role. Since the samples

were non-oriented it was not possible to distinguish experimentally between these possibilities.

Finally, calculations on polyacetylene [45] using the same method as applied here have shown that the occupied π valence bands have a width of about 5–6 eV for both *trans* and *cis* polyacetylene in agreement with most other theoretical studies of polyacetylene. Since our calculations show that carbon p functions are important for all π valence bands for polythiophene, the corresponding width in figure 3 is the total π valence band width, i.e. about 8 eV Therefore, since the lowering of symmetry upon passing from *trans* to *cis* polyacetylene leads to only modest changes in the width, we would expect similar modest changes for a polyacetylene structure as that for polythiophene, but with every sulphur atom replaced by two non-interacting hydrogen atoms. The observed roughly 50% increase in the width for polythiophene must therefore be ascribed the presence of the sulphur atoms.

We will now focus on the π orbitals closest to the Fermi level and in the next section present a model for those. In section 5 we will use this in examining solitons and polarons.

4. A model Hamiltonian

In the model by Su *et al* [8,9] only carbon π orbitals are treated within a tight-binding (Hückel) Hamiltonian whereas the remaining part of the total energy is written as

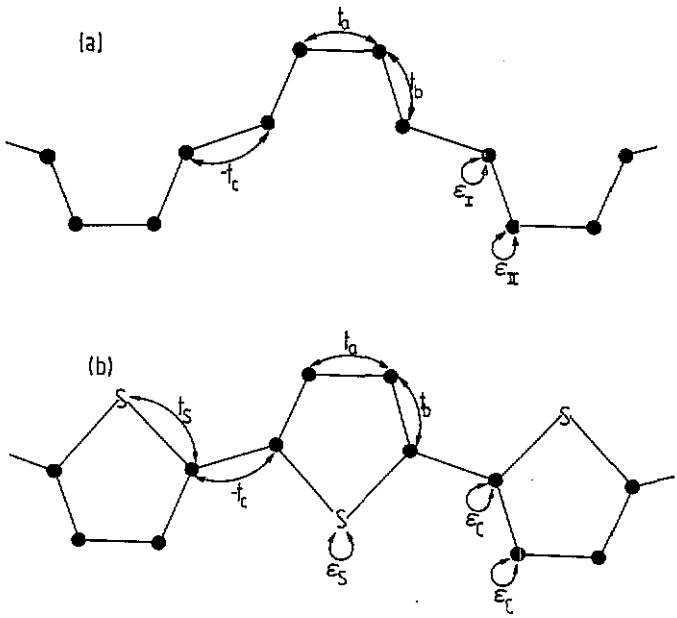

Figure 5. Schematic representation of two different tight-binding models for the π electrons of polythiophene. t denote hopping integrals and ϵ on-site terms. In (*a*) is the presence of the sulphur atoms solely included via two different carbon on-site terms ($\epsilon_I \neq \epsilon_{II}$), whereas in (*b*) all carbon atoms have the same on-site terms (ϵ_C) but the sulphur atoms are directly taken into account. Since the π functions of neighbouring C_4H_2S units are antiparallel, the hopping integrals t_c have been given a prefactor -1.

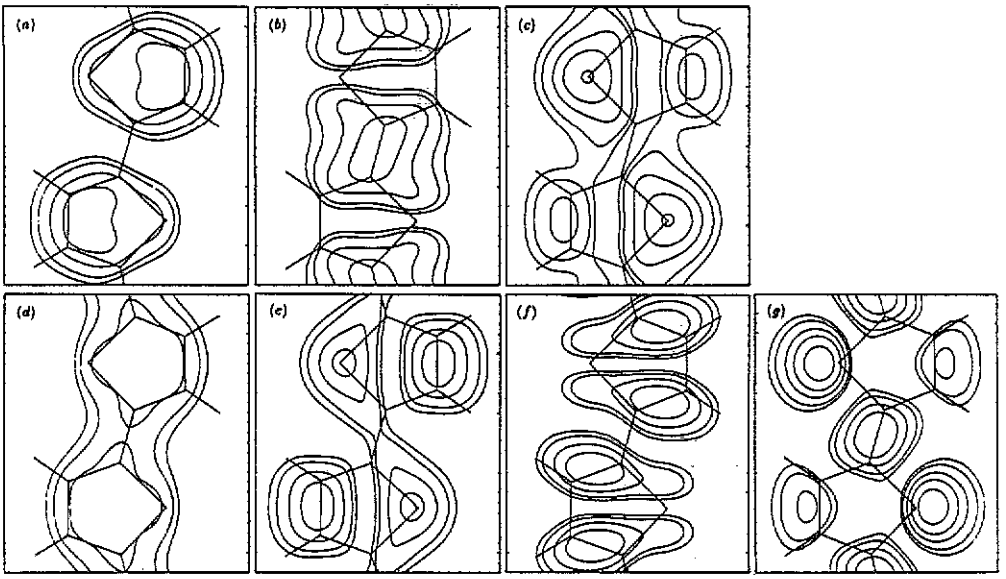

Figure 6. Contour plots of the electron densities of the π orbitals of polythiophene as obtained from the first-principles calculations for $\delta = 0$. They are shown in a plane parallel to that of the nuclei but 2 au away from it. Refering to figure 3 the orbitals are ((*a*), (*d*)) the π_1, ((*b*), (*e*)) the π_2, and ((*c*), (*e*)) the π_3 valence orbitals and (*g*) the π_4 conduction orbital at the zone centre ($k = 0$, (*a*)–(*c*)) and the zone edge ($k = 1$, (*d*)–(*g*)). The size of the planes is 12 x 14 au, the contour values are 0.001, 0.002, 0.005, 0.01, and 0.02 au, and the underlying nuclear backbone (cf figure 1) is sketched for improving the clarity.

a simple function of the coordinates of the carbon nuclei. It is often assumed that this model—perhaps with smaller modifications—also can be used for other polymers, such that only carbon-centred π orbitals need to be treated explicitly.

We have previously [46] examined such a model qualitatively. For polythiophene we studied the π electron spectra for a tight-binding model as that depicted schematically in figure 5(*a*). The presence of the sulphur atoms was modelled by extra on-site terms for the carbon atoms neighbouring the sulphur atoms (i.e. $\epsilon_{II} \neq \epsilon_I$ in figure 5(*a*)). Three interatomic carbon–carbon hopping integrals were used and they were assumed to depend linearly on the corresponding bond lengths. We demonstrated that only under special circumstances would solitons induce electronic energy levels close to the mid-gap position. As mentioned in the introduction, a soliton is a domain wall separating the A and the B phases, and from studies of some simple systems we have suggested [47] that only when the band gap vanishes for a certain periodic structure with bond-order alternation between those of the A and B phases, a soliton will induce a state close to the mid-gap position. This is obviously the case for *trans* polyacetylene but the situation is less clear for polythiophene for which we in the present study do not find a band-gap closure for the transition between the aromatic and quinoid structure but where the more complicated structure as well as the presence of the sulphur atoms might lead to modifications in the above-mentioned suggestion. It should be added that in our earlier qualitative model [46] we did indirectly assume such a band-gap closure and found, in agreement with our criterion, that a soliton induces a near-mid-gap state.

We first examine whether a tight-binding description of the π electrons of polythiophene including solely orbitals on the carbon sites is a good approximation. To this end we show in figure 6 contour plots of the electron densities of the π orbitals.

The orbitals of the π_1 band (figures 6(*a*) and 6(*d*)) are seen to be localized mainly on the carbon backbone, but with some sulphur p components. As above we consider a hypothetical π_2(small k) + π_3(large k) band and a hypothetical π_2(large k) + π_2(small k) band. The latter (figures 6(*c*) and 6(*e*)) has both sulphur and carbon p components in agreement with the results of Fujimoto *et al* [38,39], whereas the former (figures 6(*b*) and 6(*f*)) besides carbon p components also has important contributions from sulphur d functions. Finally, the lowest-lying π conduction orbitals (figure 6(*g*)) are mostly constructed from both sulphur and carbon p functions.

Figure 6 demonstrates the already mentioned importance of sulphur d functions in the present first-principles approach as well as the fact that sulphur components are found in the whole energy region spanned by the π bands. Therefore, due to the results of figure 6 we find that a realistic model must include sulphur-centred π orbitals, but in order to simplify the model we will here not distinguish between p and d functions but only include one type of sulphur-centred function. Neglecting next-nearest neighbour interactions we thus arrive at the model sketched in figure 5(*b*), which has similarities with that used by Bertho *et al* [48–50].

As is common practice we introduce configuration coordinates $\{u_n\}$ with u_n being the position of the nth carbon atom relative to that in the perfect, undistorted, 'undimerized' structure with $\delta = 0$ (see figure 7). We also define

$$\phi_n = (-1)^n u_n \,. \tag{2}$$

With the numbering of the atomic sites shown in figure 7 the carbon–carbon and carbon–sulphur bond lengths are assumed as follows:

$$\begin{aligned}
d(4m, 4m+1) &= d_c + \delta_c(\phi_{4m+1} + \phi_{4m}) \\
d(4m+4, 4m+5) &= d_c + \delta_c(\phi_{4m+5} + \phi_{4m+4}) \\
d(4m+1, 4m+2) &= d_b - \delta_b(\phi_{4m+2} + \phi_{4m+1}) \\
d(4m+3, 4m+4) &= d_b - \delta_c(\phi_{4m+4} + \phi_{4m+3}) \\
d(4m+2, 4m+3) &= d_a + \delta_a(\phi_{4m+3} + \phi_{4m+2}) \\
d(4m+1, S_m) &= d_S \\
d(4m+4, S_m) &= d_S \,.
\end{aligned} \tag{3}$$

Here, d_a, d_b, d_c, d_S, δ_a, δ_b, and δ_c are constants chosen such that for $\phi_n = \phi_0 = +0.5$ and $\phi_n = \phi_0 = -0.5$ the aromatic and the quinoid structure, respectively, of equation (1) are obtained. Thus, $d_a = d_c = 2.645$ au, $d_b = 2.695$ au, $\delta_a = \delta_b = \delta_c = 0.085$ au, and $d_S = 3.245$ au.

Analogously to equation (3), the hopping integrals (t) are linearized in the parameters $\{\phi_n\}$, i.e.

$$t(4m, 4m+1) = t_{c0} - \alpha_c(\phi_{4m+1} + \phi_{4m}) \tag{4}$$

etc. Furthermore, carbon and sulphur on-site terms (ϵ_C and ϵ_S) are introduced. The tight-binding Hamiltonian is thus (see figure 5(*b*)):

$$\hat{H}_\pi = \sum_s \sum_m \left\{ \left[\epsilon_S c^\dagger_{S_m,s} c_{S_m,s} + \sum_{l=1}^{4} \epsilon_C c^\dagger_{4m+l,s} c_{4m+l,s} \right] \right.$$

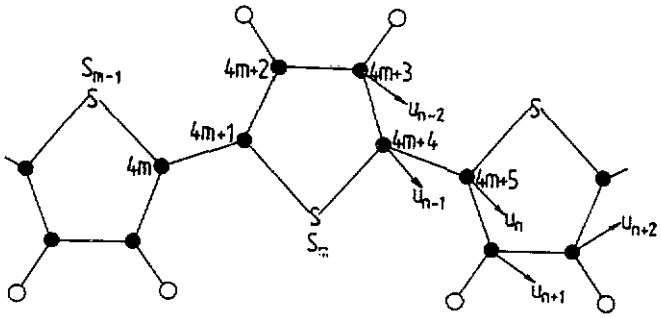

Figure 7. The numbering of the sites used in the model Hamiltonian. m labels the unit cell, $4m+1$, $4m+2$, $4m+3$, and $4m+4$ the carbon sites and S_m the sulphur site in the unit cell. Also shown are configuration coordinates u_n.

$$-\left[t_{S0}\left(c^{\dagger}_{4m+1,s}c_{S_m,s}+c^{\dagger}_{S_m,s}c_{4m+1,s}+c^{\dagger}_{4m+4,s}c_{S_m,s}+c^{\dagger}_{S_m,s}c_{4m+4,s}\right)\right.$$
$$+\sum_{l=1}^{4}t(4m+l,4m+l+1)$$
$$\left.\times\left(c^{\dagger}_{4m+l+1,s}c_{4m+l,s}+c^{\dagger}_{4m+l,s}c_{4m+l+1,s}\right)\right]\Bigg\} \qquad (5)$$

where s is a spin variable, m labels the thiophene units, l labels the carbon sites in one unit cell, and $c^{\dagger}_{x,s}$ and $c_{x,s}$ are the creation and annihilation operators, respectively, of a π electron with spin s on site x.

The values of the parameters were obtained by fitting the first-principles π_1, π_2, and π_3 valence bands for the periodic structures with $\phi_n = \phi_0 = -0.6, -0.5, \ldots, 0.6$. The fit resulted in the following parameter values: $\epsilon_C = -3.20$ eV, $\epsilon_S = -5.03$ eV, $t_{a0} = 3.48$ eV, $t_{b0} = 3.27$ eV, $t_{c0} = 2.94$ eV, $t_{S0} = 1.93$ eV, $\alpha_a = 0.307$ eV, $\alpha_b = 0.047$ eV, and $\alpha_c = 0.284$ eV. Before discussing these values it should be stressed that correlation among the parameters easily results in a situation where certain large simultaneous shifts in all parameter values produce fits of almost unchanged quality. Keeping this in mind we notice, however, that in agreement with general results [51] the carbon–sulphur hopping integrals are smaller than those of carbon–carbon bonds. Moreover, accurate, fully numerical, self-consistent solutions of the Kohn–Sham equations for isolated atoms give single-particle eigenvalues equal to -7.6 eV and -5.9 eV for sulphur 3p and carbon 2p electrons, respectively. Our parameters show about the same difference ($\epsilon_C - \epsilon_S$), but the absolute values have been shifted by 2–3 eV in accordance with the difference between our calculated ionization potential and the experimental one (see, e.g. table 1). The carbon–carbon hopping integrals are slightly larger than those used for *trans* polyacetylene by Su *et al* [8,9].

Let us finally compare the values of equation (8) with those obtained by a similar procedure for polyvinylene sulphide [36]. For this we found $\epsilon_C - \epsilon_S \simeq 1.5$ eV and $t_{S0} \simeq 3.0$ eV, whereas typical C–C hopping integrals were found slightly smaller. The results for polythiophene and those for polyvinylene sulphide thus differ mainly in the size of the carbon–sulphur hopping integrals, indicating that the sulphur atoms are less important for the transport properties for polythiophene than for polyvinylene sulphide.

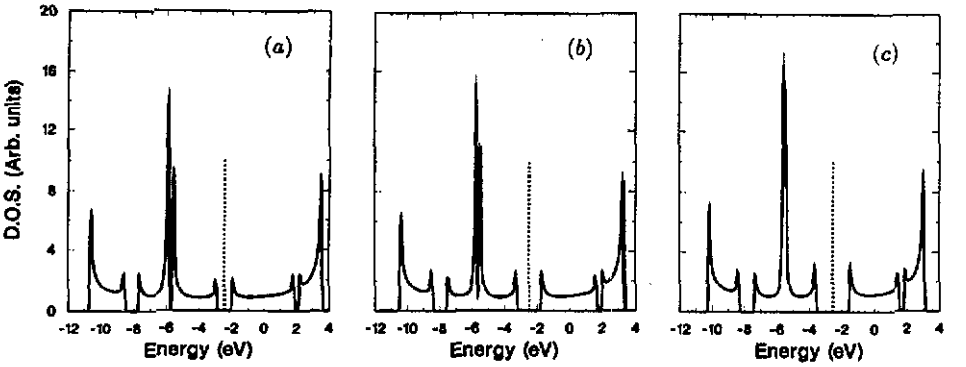

Figure 8. π electron density of states calculated for the periodic, infinite chains with $\phi_n = \phi_0 = -0.5$ ((*a*): the quinoid case), 0.0 ((*b*): the 'undimerized' case), and $+0.5$ ((*c*): the aromatic case) as calculated with the tight-binding model Hamiltonian $\hat{H}_\pi$. The vertical broken lines represent the Fermi level for the neutral polymer. The curves have been obtained for periodic ring molecules of 100 thiophene units and the discrete energy levels have been broadened with Gaussians of FWHM (full width at half maximum) equal to 0.1 eV.

The total Hamiltonian is now assumed written as a sum of the tight-binding part $\hat{H}_\pi$ and a remainder $\hat{H}_\sigma$:

$$\hat{H} = \hat{H}_\pi + \hat{H}_\sigma \,. \tag{6}$$

As is common practice, $\hat{H}_\sigma$ is approximated by a simple function of the configuration coordinates $\{\phi_n\}$, and by writing it as

$$\hat{H}_\sigma = \sum_m \sum_l \left[\sum_{i=1}^{4} K_i (\phi_{4m+l+1} + \phi_{4m+l})^i \right] \tag{7}$$

the constants K_i can be determined such that both the quinoid ($\phi_n = \phi_0 = -0.5$) and the aromatic ($\phi_n = \phi_0 = +0.5$) structures correspond to (meta-)stable structures for the neutral, undistorted polymer, and such that the 'dimerization' energies (i.e. the differences in the total energy of the aromatic or quinoid structure and that of the 'undimerized' structure with $\phi_n = \phi_0 = 0$) have pre-defined values. But due to the restricted geometry variations in the first-principles calculations our information about the total energy as a function of nuclear coordinates are too limited to be used in determining K_i, and we have therefore chosen to focus solely on the π electrons, i.e. on $\hat{H}_\pi$.

We have modelled the infinite polythiophene chain by a ring molecule of either $N = 40$ or $N = 100$ thiophene units, thereby imposing periodic boundary conditions and avoiding end effects. Since the results for $N = 40$ and for $N = 100$ differed only insignificantly a ring of $N = 40$ units can be considered a good approximation to an infinite chain.

In figure 8 we show the density of states for the perfect, periodic chain with $\phi_n = \phi_0$ for $\phi_0 = -0.5$, for $\phi_0 = 0$, and for $\phi_0 = +0.5$ as obtained with the model Hamiltonian of equation (6). The $\phi_0 = 0$ case (figure 8(*b*)) corresponds to figures 3 and 4, and a direct comparison is thus possible. Figure 8 indicates—as

Table 2. Results of model calculations for the perfect undistorted chain with $\phi_n = \phi_0 = 0$. Listed are the squares of the coefficients to the basis functions at the C_α sites (the carbon sites neighbouring sulphur atoms), the C_β sites (the carbon atoms not being neighbours to sulphur atoms), and the sulphur sites (S). The band and k variable refer to figure 3, and the label to that part in figure 6, which depicts the electron density for the same orbital but obtained from the first-principles calculations. The coefficients are normalized to be 1 for the largest one, and it is noted that the sulphur components for the $\pi_2(k = 0)$ and the $\pi_3(k = 1)$ orbitals are identically 0 due to symmetry (cf figure 6).

Band	k	C_α	C_β	S	Label
π_1	1	1.0	0.8	0.5	*(d)*
π_1	0	0.3	1.0	0.4	*(a)*
π_2	0	1.0	0.2	0	*(b)*
π_2	1	< 0.1	0.4	1.0	*(e)*
π_3	0	< 0.1	0.1	1.0	*(c)*
π_3	1	1.0	0.8	0	*(f)*
π_4	1	0.7	0.3	1.0	*(g)*

also found in the first-principles calculations—that no band-gap closure occurs for the quinoid-to-aromatic transition according to the model calculations.

In table 2 we list the squares of the coefficients to the basis functions of different sites found in the model calculations for $\phi_n = \phi_0 = 0$. Since the basis functions in the tight-binding model are assumed orthonormal the numbers in the table are proportional to Mulliken populations. Table 2 can readily be compared with figure 6, and we see that not only the position of the bands but also their nature is well represented by the model except for the orbitals which according to the first-principles calculations have large sulphur d components. The results suggest therefore that descriptions without the inclusion of sulphur d functions can give realistic energy bands, although the nature of the orbitals can be related with some uncertainty.

In the following section we will apply the model to study the position of soliton- and polaron-induced gap-states. Due to the lack of parameters for $\hat{H}_\sigma$ we do not attempt to study the (relative) stability of the solitons and polarons. Before doing so we will, however, like to point out some of the limitations of the model.

First of all, the parameters and the model have been derived by examining neutral, periodic, infinite chains, and extra terms due to symmetry-lowering and/or charging have therefore not been considered. Neither have correlation effects, inter-chain couplings, nor finite-size effects nor effects due to spin polarizations. Furthermore, the 'true' quinoid and aromatic structures will most likely be slightly different to those examined here, such that the changes in the π bands under the aromatic-to-quinoid transition will be different. Two features of the first-principles calculations will turn out to be important for the study of solitons and polarons, namely the lack of a band-gap closure for the aromatic-to-quinoid transition and the relative position of the Fermi levels in the neutral aromatic and quinoid structures. We believe the variations in the size of the gap to be largely determined from the variations in the carbon–carbon hopping integrals as functions of the bond-length alternation, and since these will change only modestly upon reasonable changes in the geometry, we find that an unrealistically large bond-length alternation is required in order to close the gap. Therefore, we consider the lacking band-gap closure a true effect. On the other hand, different realistic quinoid and aromatic structures might easily have band

gaps whose positions are shifted some few tenths of an eV relative to those used here. The relative position of the Fermi levels for the two structures is therefore connected with some uncertainty. This might result in non-negligible modifications in the position of the gap states induced by the solitons and polarons. In the following section we will try to estimate the consequences of modifying the relative positions of the Fermi levels for the undistorted structures.

5. Solitons and polarons

In the very special (and unlikely) case that the total energies of the quinoid and the aromatic structures are identical, solitons as schematically depicted in figure 1(*c*) might be (meta-)stable distortions of the neutral or charged polymer.

In figure 9 we show the calculated π electron density of states for a chain containing a soliton–antisoliton pair. The configuration coordinates ϕ_n are assumed obeying

$$\phi_n = \phi_0 \tanh \frac{n+d+\Delta}{L} \tanh \frac{n+d-\Delta}{L}. \tag{8}$$

Here L is the width of the (anti-)soliton, and $0 \leqslant d \leqslant 1$ describes the position of the nodes of the soliton and antisoliton such that upon varying d from 0 to 1 the propagation of the lattice distortion can be modelled. 2Δ is the separation between the soliton and the antisoliton, which for the non-interacting soliton–antisoliton pair is chosen equal to half the length of the ring molecule. In figure 9 we have chosen $d = 0.5$ and $L = 0.01$, but other values of d and L were found to lead to results differing only very little from those of figure 9.

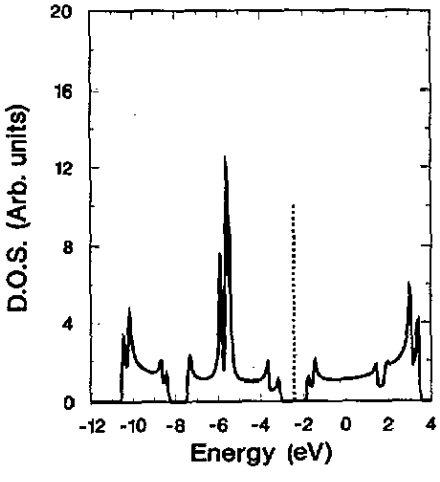

Figure 9. As figure 8 but for a ring with a well-separated soliton–antisoliton pair, such that half of the molecule is quinoid and the other half aromatic.

We notice at once the absence of a near-mid-gap state and comparing with figure 8 the spectrum of figure 9 resembles two overlapping spectra of the quinoid and the aromatic isomer (figure 8(*a*) and 8(*c*), respectively). The first finding is in accordance with the requirement of a band-gap closure under the transition between the A and the B phases for obtaining soliton-induces states close to the mid-gap position.

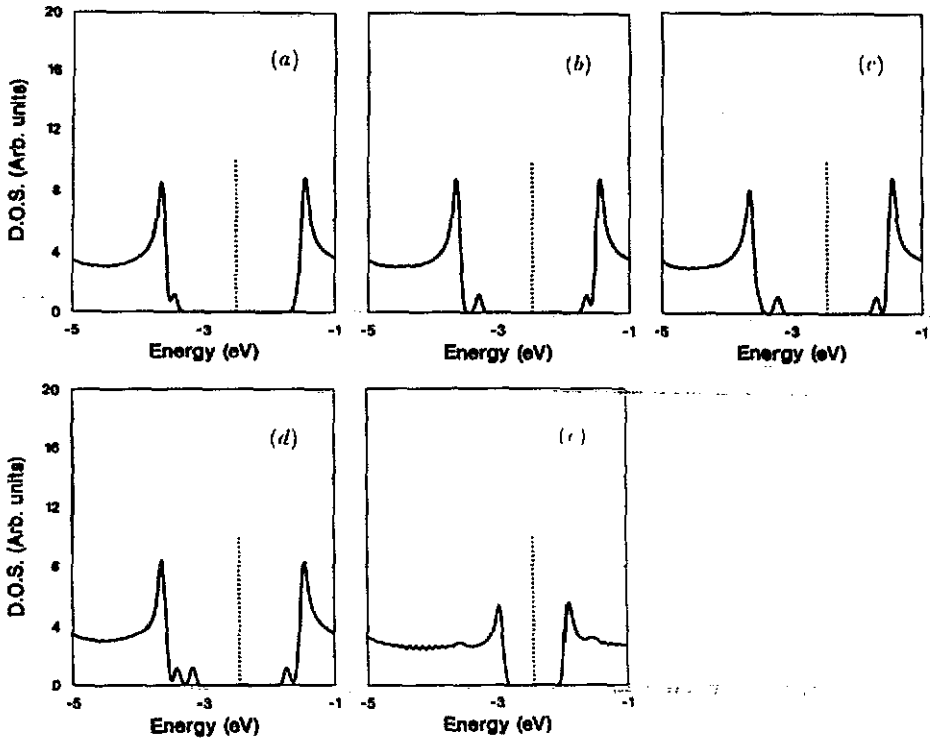

Figure 10. As figure 8 but for a chain containing a soliton–antisoliton pair. In (*a*)–(*d*) the pair is inserted into the aromatic structure, in (*e*) into the quinoid structure. The distance between the soliton and the antisoliton is in (*a*) 2.5, in (*b*) 5.0, in (*c*) 7.5, and in (*d*) and (*e*) 10.0 thiophene units.

When studying the electronic densities of the various orbitals it is found that none of the orbitals near the Fermi level for the neutral polymer are localized close to the nodes of ϕ_n, in contrast to the results for *trans* polyacetylene, but instead are spread out over the whole polymer or localized to either the quinoid or the aromatic part. Thus, we do not find any so-called interface states. Also this finding can be related to the lacking band-gap closure [46].

When reducing Δ in equation (8) a polaron is formed. In figure 10 we show the resulting density of states. For $\phi_0 > 0$ we see that when Δ is increased from 5 (figure 9(*a*)) to 20 (figure 9(*d*)) more extra states appear in the gap. On the other hand, when changing the sign of ϕ_0 no gap states are found (figure 10(*e*)), but instead a careful inspection reveals extra weak peaks at the positions of the band edges of the aromatic compound.

Besides their presence in figures 10(*a*)–(*d*) we also note that the position of the gap states is not symmetric in the gap. This is in contrast to the results of the simplest tight-binding model for *trans* polyacetylene but might be the subject to some modifications when the position of the quinoid gap relative to the aromatic gap is changed. We finally mention that the spectra of figure 10 are very insensitive to the values of d and L.

For a doped polymer with low dopant concentration singly or doubly charged,

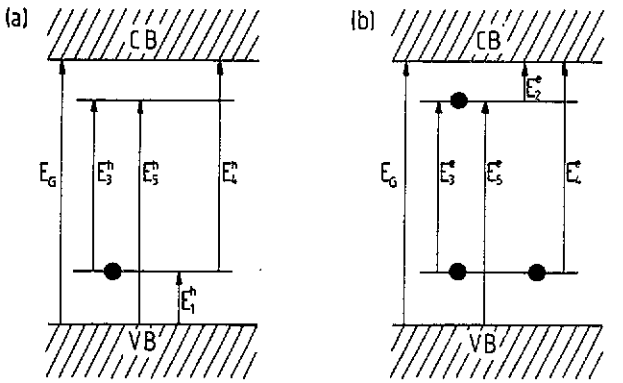

Figure 11. Schematic representation of the energy levels of a singly positively (*a*) and negatively (*b*) charged chain containing a polaron. VB and CB denotes the valence band and the conduction band, respectively. The two gap levels can each contain two electrons and their occupancies are shown as the number of full circles. The vertical arrows represent the possible low-energy electronic excitations.

non-interacting polarons are believed to be created in the polymer chain. In figure 11 we show schematically the energy levels and their occupancies for a singly charged polaron when its charge is positive (a hole polaron, figure 11(*a*)) and when it is negative (an electron polaron, figure 11(*b*)). Also shown are the possible electronic excitations for energies up to the gap E_G. In the case of doubly charged polarons (bipolarons) the gap states are either completely empty or completely filled, and for those will the transitions E_3^h, E_4^h, E_3^e, and E_5^e disappear.

As is evident from figures 10(*a*)–(*d*) and figure 9, more and more states appear in the gap as Δ is increased. It is, however, unlikely that Δ is so large that more than two asymmetric gap levels appear since only those deepest in the gap will change population upon doping.

It turned out that for not too large Δ ($\Delta \leqslant 15$) E_1 and E_2 depend approximately linearly on Δ:

$$E_1 \simeq 0.031 \text{ eV} \times \Delta \qquad E_2 \simeq 0.018 \text{ eV} \times \Delta \,. \tag{9}$$

Using figure 11 and $E_G = 1.98$ eV the other transition energies as functions of Δ can easily be found.

Brédas and co-workers [24] have examined sodium-doped polythiophene using the VEH method. Thereby the effects of the dopants were directly included in contrast to our model, but on the other hand only one type of dopant was considered, and the calculations were semi-empirical. They found $E_1 = 0.61$ eV and $E_2 = 0.71$ eV, i.e. $E_1 < E_2$ in contrast to our findings. Stafström and Brédas [52] have later examined positively charged isolated polythiophene chains containing polarons or bipolarons also within the VEH framework. They found for polarons $E_1 = 0.32$ eV and $E_2 = 0.47$ eV and for bipolarons $E_1 = 0.57$ eV and $E_2 = 0.73$ eV The values are slightly different to those mentioned above but still E_1 is found to be smaller than E_2.

On the other hand, the model calculations by Bertho and Jouanin [48] led to $E_1 > E_2$ in agreement with our results. For various charges they found optimized structures with (E_1, E_2) = (0.36, 0.28) eV, (0.74, 0.57) eV, (0.29, 0.17) eV, and (0.53, 0.42) eV, which actually agree fairly well with our empirical equation (9).

Harbeke *et al* [53] have reported experimentally derived optical spectra of polythiophene and poly-3-methylthiophene doped with BF_4^-. The observed transitions are to be compared with those of figure 11(*a*). The most detailed results were reported for poly-3-methylthiophene for which they found a peak at 0.5 eV and a broad band between 1.2 eV and 1.6 eV. For polythiophene a peak at 0.8 eV and a broad band between 1.4 and 1.9 eV were observed. Interpreting the lowest peaks as due to E_1^h results in a fairly large value of Δ: $\Delta > 15$–20, in which case $E_3^h < 1.2$ eV, $E_4^h < 1.5$ eV, and $E_5^h < 1.7$ eV. The lack of a peak below 1.2 eV seems, therefore, to imply the lack of an E_3^h transition and hence that the charge carriers are bipolarons and not polarons.

Photo-induced polarons in polythiophene and poly-3-methylthiophene have been studied by Kaneto *et al* [54, 55]. Here both hole and electron polarons (as well as neutral polarexcitons) are induced and an interpretation is accordingly more difficult since the internal structures of hole and electron polarons need not be identical. For polythiophene the results show peaks at about 0.8 eV, 1.3 eV, 1.6 eV, and 1.9 eV. Also here the lack of peaks around 1.0–1.2 eV indicates lacking E_3^e and E_3^h transitions in agreement with a model in which bipolarons are the generated quasi-particles.

Colaneri *et al* [56] have reported optical spectra of positively charged poly-3-methylthiophene. Their findings of peaks at roughly 0.65 eV and 1.6 eV are consistent with the picture in which bipolarons and not polarons are the charge carriers as also proposed by Colaneri *et al*. Finally, Rühe *et al* [57] have reported experimental results on photo-excited alkyl-substituted polythiophenes. Also they are lacking a transition at about 1 eV, but whereas they ascribe the observed asymmetry between the gap states correlation effects, we have shown here that single-particle effects can also be responsible for this.

Our interpretation of the optical spectra is not unique as indicated at the end of the preceeding section. First of all, our model has been derived by considering only a limited number of infinite, periodic structures. Moreover, both correlation effects and effects disappearing for the periodic structures might be of importance for the charged and/or symmetry-lowered chain. On the other hand, also modifying the model such that the polaron-induced states appear symmetric in the gap will not change the conclusions. The variations in the hopping integrals as functions of bond lengths will only change slightly when modifying the quinoid-to-aromatic transition. A model for which the polaron-induced gap states appear symmetric in the gap could be like

$$E_1 = E_2 = 0.025 \text{ eV} \times \Delta \tag{10}$$

replacing equation (9). Also, this model would give $\Delta > 15$–20, and hence $E_3 < 1.2$ eV, which remains outside the range of the experimental peaks, still implying that bipolarons and not polarons are created in charged or excited polythiophene.

The large values of Δ might be considered related to a repulsion between each half of the soliton–antisoliton pair. However, for $\Delta > 15$ more states appear in the gap (cf figure 10), which we consider unrealistic, and we therefore suggest that correlation effects modify the results without changing the general conclusion that Δ is large. That Δ is found to be large is in agreement with earlier studies. Bertho *et al* [48, 50] reported values of Δ of around 8. Stafström and Brédas [52] found that the optimized structures of polarons had $\Delta < 5$, whereas bipolarons were characterized by larger values of Δ. Combining this with our results we find this a further indication that bipolarons are the generated quasi-particles.

We finally mention that Lögdlund *et al* [58] have reported that the Fermi level of poly(3-hexylthiophene) heavily doped with $NOPF_6$ is lowered compared with the undoped compound and that there is a finite density of states at the Fermi level. This was interpreted as indicating the formation of a polaron lattice. Our results suggest that at low dopant concentrations bipolarons are formed. However, they are so delocalized that for moderate dopant concentrations they will interact. The results of Lögdlund *et al* suggest, then, that this interaction stabilizes polarons in preference to bipolarons.

6. Conclusions

We have studied periodic, infinite, planar chains of polythiophene with the first-principles, density-functional, full-potential, LMTO method for helical polymers. We have concentrated on the electronic orbitals and eigenvalues and how they change under an aromatic-to-quinoid transition. Except for a likely downwards shift of the σ levels relative to the π levels of about 1 eV the band structures were found to be realistic and offered a consistent interpretation of experimental photoelectron spectra. The band gap was found to decrease—but not to vanish—when passing from the aromatic to the quinoid isomer. Finally, it was found that sulphur d functions were non-negligible in the calculations.

We have proposed a tight-binding model that could describe the π electrons of the compound. With this we have studied the π electron density of states for chains containing solitons and polarons. The solitons were found not to induce near-mid-gap levels, and for polarons the gap levels were found to lie highly asymmetrically in the gap. Although the model suffered from some limitations (e.g. the lack of finite-size effects, of correlation effects, and of interchain interactions), and was closely connected with the assumption that the π electron spectra changed exactly as prescribed under the specific aromatic-to-quinoid transitions, a comparison with experimental photoabsorption spectra indicated that the doping- or photo-induced distortions are bipolarons and not polarons in the dilute limit, and that the soliton and antisoliton forming a bipolaron are well separated.

Acknowledgment

This work was partly supported by the Danish Natural Science Research Council.

References

[1] *Proc. Int. Conf. Sci. Technol. Synthetic Metals (Santa Fe) 1988* (*Synth. Metals* 27–29) 1988–89
[2] Chiang C K, Fincher Jr C R, Park Y W, Heeger A J, Shirakawa H, Louis E J, Gau S C and MacDiarmid A G 1977 *Phys. Rev. Lett.* **39** 1098
[3] Kaneto K, Yoshino K and Inuishi Y 1983 *Solid State Commun.* **46** 389
[4] Waltman R J, Bargon J and Diaz A D 1983 *J. Phys. Chem.* **87** 1459
[5] Yumoto Y and Yoshimura S 1986 *Synth. Metals* **13** 185
[6] Kobayashi M, Chen J, Chung T-C, Moraes F, Heeger A J and Wudl F 1984 *Synth. Metals* **9** 77
[7] Elsenbaumer R L, Jen K Y and Oboodi R 1986 *Synth. Metals* **15** 169
[8] Su W P, Schrieffer J R and Heeger A J 1979 *Phys. Rev. Lett.* **42** 1698
[9] Su W P, Schrieffer J R and Heeger A J 1980 *Phys. Rev.* B **22** 2099; 1983 *Phys. Rev.* B **28** 1138(E)
[10] Brédas J L, Chance R R and Silbey R 1981 *Mol. Cryst. Liq. Cryst.* **77** 319
[11] Brazovskiĭ S A and Kirova N N 1981 *Pis'ma Zh. Eksp. Teor. Fiz.* **33** 6 (1981 *JETP Lett.* **33** 4)
[12] Campbell D K and Bishop A R 1981 *Phys. Rev.* B **24** 4859

[13] Springborg M and Andersen O K 1987 *J. Chem. Phys.* **87** 7125
[14] Springborg M 1989 *J. Chim. Physique* **86** 715
[15] Hohenberg P and Kohn W 1964 *Phys. Rev.* B **136** 864
[16] von Barth U and Hedin L 1972 *J. Phys. C: Solid State Phys.* **5** 1629
[17] Kohn W and Sham L J 1965 *Phys. Rev.* A **140** 1133
[18] Löwdin P-O 1970 *Adv. Quantum Chem.* **5** 185
[19] Lee Y-S and Kertész M 1988 *J. Chem. Phys.* **88** 2609
[20] Mintmire J W, White C T and Elert M L 1988 *Synth. Metals* **25** 109
[21] Brédas J L, Elsenbaumer R L, Chance R R and Silbey R 1983 *J. Chem. Phys.* **78** 5656
[22] Bakhshi A K, Ladik J and Seel M 1987 *Phys. Rev.* B **35** 704
[23] Brédas J L, Street G B, Thémans B and André J M 1985 *J. Chem. Phys.* **83** 1323
[24] Brédas J L, Thémans B, Fripiat J G, André J M and Chance R R 1984 *Phys. Rev.* B **29** 6761
[25] Thémans B, André J M and Brédas J L 1987 *Synth. Metals* **21** 149
[26] Riga J, Snauwaert Ph, de Pryck A, Lazzaroni R, Boutique J P, Verbist J J, Brédas J L, André J M and Taliani C 1987 *Synth. Metals* **21** 223
[27] Taliani C, Zamboni R, Danieli R, Ostoja P, Porzio W, Lazzaroni R and Brédas J L 1989 *Phys. Scr.* **40** 781
[28] Otto P and Ladik J 1990 *Synth. Metals* **36** 327
[29] Tanaka K, Wang S and Yamabe T 1989 *Synth. Metals* **30** 57
[30] Tourillon G and Jugnet Y 1989 *J. Chem. Phys.* **89** 1905
[31] Cui C X and Kertész M 1989 *Phys. Rev.* B **40** 9661
[32] Mintmire J W, White C T and Elert M L 1986 *Synth. Metals* **16** 235
[33] Onoda M, Manda Y, Yokoyama M, Sugimoto R and Yoshino K 1989 *J. Phys.: Condens. Matter* **1** 3859
[34] Springborg M and Jones R O 1986 *Phys. Rev. Lett.* **57** 1145
[35] Springborg M and Jones R O 1988 *J. Chem. Phys.* **88** 2652
[36] Springborg M 1989 *Synth. Metals* **32** 337
[37] Wu C R, Nilsson J O, Inganäs O, Salaneck W R, Österholm J-E and Brédas J L 1987 *Synth. Metals* **21** 197
[38] Fujimoto H, Nagashima U, Inokuchi H, Seki K, Nakahara N, Nakayama J, Hoshino M and Fukuda K 1990 *Phys. Scr.* **41** 105
[39] Fujimoto H, Nagashima U, Inokuchi H, Seki K, Cao Y, Nakahara N, Nakayama J , Hoshino M and Fukuda K 1990 *J. Chem. Phys.* **92** 4077
[40] Derrick P J, Åsbrink L, Edqvist O, Jonsson B-Ö and Lindholm E 1971 *Int. J. Mass. Spectrosc. Ion Phys.* **6** 177
[41] Gelius U, Allan C J, Johansson G, Siegbahn H, Allison D A and Siegbahn K 1971 *Phys. Scr.* **3** 237
[42] Gelius U, Roos B O and Siegbahn P 1972 *Theor. Chim. Acta (Berlin)* **27** 171
[43] Fink J, Nücker N, Scheerer B and Neugebauer H 1987 *Synth. Metals* **18** *163*
[44] Fink J 1989 *Adv. Electr. Electron Phys.* **75** 121
[45] Springborg M 1986 *Phys. Rev.* B **33** 8475
[46] Springborg M, Kiess H and Hedegård P 1989 *Synth. Metals* **31** 281
[47] Springborg M 1989 *Physica* B **172** 225
[48] Bertho D and Jouanin C 1987 *Phys. Rev.* B **35** 626
[49] Bertho D and Jouanin C 1988 *Synth. Metals* **24** 179
[50] Bertho D, Laghdir A and Jouanin C 1988 *Phys. Rev.* B **38** 12531
[51] Streitwieser Jr A 1961 *Molecular Orbital Theory for Organic Chemists* (New York: Wiley)
[52] Stafström S and Brédas J L 1988 *Phys. Rev.* B **38** 4180
[53] Harbeke G, Baeriswyl D, Kiess H and Kobel W 1986 *Phys. Scr.* T **13** 302
[54] Kaneto K, Uesugi F and Yoshino K 1987 *J. Phys. Soc. Japan* **56** 3703
[55] Kaneto K, Uesugi F and Yoshino K 1987 *Solid State Commun.* **64** 1195
[56] Colaneri N, Nowak M, Spiegel D, Hotta S and Heeger A J 1987 *Phys. Rev.* B **36** 7964
[57] Rühe J, Colaneri N F, Bradley D D C, Friend R H and Wegner G 1990 *J. Phys.: Condens. Matter* **2** 5465
[58] Lögdlund M, Lazzaroni R, Stafström S, Salaneck W R and Brédas J-L 1989 *Phys. Rev. Lett.* **63** 1841